Chapter 54
Sliding Abrasive and Adhesive Wear Behavior of TIG-Cladded NiTi–W Coating Deposited on Ti–6Al–4V Alloy

Jyotirmoy Singh Garbyal, Chinmaya Kumar Padhee, Abdu Raheem and Manoj Masanta

Abstract The wear characteristic of NiTi–W composite layer developed on Ti–6Al–4V alloy by using TIG cladding route was evaluated. The NiTi–W composite coating fabricated with preplaced Ni–Ti–W powder with 9:9:2 weight ratio and at 60 A current and 2.3 mm/s scan speed has been tested against an abrasive disk and hardened steel (HRC 58) under different normal load and sliding velocity conditions to analyze its sliding abrasive wear and adhesive wear behaviors. The effect of test conditions on the wear characteristic of the NiTi–W clad layer was analyzed in-depth and compared with the wear characteristic of the uncoated Ti–6Al–4V alloy. It was found that the NiTi–W composite coating shows up to eleven times better wear resistance than the uncoated Ti–6Al–4V alloy under abrasive wear test conditions and more than seven times under sliding adhesive test condition.

Keywords TIG cladding · NiTi–W coating · Ti–6Al–4V alloy · Wear resistance

54.1 Introduction

Titanium and its alloys find lots of applications in industries like aerospace, medical, and military due to some of its properties like specific strength, good corrosion resistance, and decent high temperature [1–3]. With the aim of reducing weight, Ti alloys are employed in spacecraft bearings instead of steel. But their relatively low surface hardness and poor wear resistance lead to a great problem in these applications [4]. An effective way to improve the surface properties of the Ti–6Al–4V alloy is the deposition of the ceramic reinforced hard coating layer by laser cladding or alloying route [5, 6]. However, laser processing is quite expensive and requires complicated arrangements. On the other hand, tungsten inert gas (TIG) cladding process stands apart due to its low-cost and easy-to-operate characteristics. It is pertinent to a range of

J. S. Garbyal · C. K. Padhee · A. Raheem · M. Masanta (✉)
Department of Mechanical Engineering, National Institute of Technology Rourkela, Rourkela 769008, India
e-mail: manoj.masanta@gmail.com

M. S. Shunmugam and M. Kanthababu (eds.), *Advances in Micro and Nano Manufacturing and Surface Engineering*, Lecture Notes on Multidisciplinary Industrial Engineering,
https://doi.org/10.1007/978-981-32-9425-7_54

materials, and the heat input can be controlled accurately by changing the processing current and scan speed [7, 8].

NiTi intermetallic alloy received enormous attention due to its shape memory and superelasticity properties in addition to its high hardness, excellent resistance to corrosion and ability to maintain stability at high temperature. Additionally, the NiTi coating is highly compatible with Ti–6Al–4V alloy [9]. Tungsten (W) is a dense metal with strength comparable to that of titanium and is also known for its high wear and corrosion resistance. Hence, it is expected that NiTi–W composite would increase the tribological properties of Ti–6Al–4V alloy substrate, without affecting its bulk properties. However, no definite work till now emphasizes the development of NiTi–W composite coating for wear-resistance applications.

The aim of this work is to analyze the wear characteristic of NiTi–W coating layer deposited on Ti–6Al–4V alloy by using the TIG cladding method. The NiTi–W composite coating layer fabricated at a specific processing condition has been tested against the abrasive disk and the hardened steel (HRC 58) disk under different normal load conditions to analyze its sliding abrasive wear and adhesive wear behaviors. The effect of test conditions on the wear behavior of the coating was analyzed in-depth and compared with the wear behavior of uncoated Ti–6Al–4V alloy.

54.2 Materials and Methodology

For the present work, TIG-cladded NiTi–W composite coating tracks deposited on Ti–6Al–4V alloy plate of 5 mm thickness were used. The deposition of the coating was performed by scanning the TIG arc on Ni–Ti–W (9:9:2 wt. ratio) pre-coated powder on Ti–6Al–4V alloy plate at 60 A current and 2.3 mm/s scan speed under atmosphere. Details of the TIG cladding procedure may be available elsewhere [10]. After the TIG cladding was done, the NiTi–W coating tracks were cut in the cylindrical shape of 4 mm diameter, so that the pin-on-disk wear test could be performed. The coated surfaces of pins were polished with polishing paper to flatten the surface and remove any oxidized layer and impurities.

The tribological tests were performed under sliding abrasive and adhesive conditions under different normal loads and sliding speeds. These are considered as variables using a pin-on-disk type tribometer as per the ASTM G99 standard. Sliding abrasive condition was created by attaching an abrasive disk on the rotating disk of the tribometer disk, and adhesive sliding wear test was done against the hardened steel disk. Figure 54.1 shows the pin-on-disk wear setup for sliding abrasive wear test and adhesive wear test arrangement. The detailed conditions for the sliding abrasive and adhesive wear tests are mentioned in Table 54.1. The wear values of the coated and the uncoated samples were assessed in terms of height loss during the wear test. The height loss due to wear was calculated from the height measurement of the pin samples before and after the test using a Vernier caliper. Additionally, the height loss of the pin samples was also noted against the test time using a data acquisition system equipped with the pin-on-disk wear test rig. After the wear test, SEM analysis on the

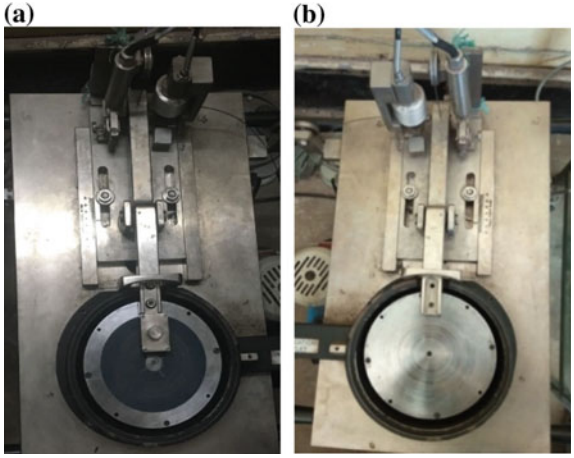

Fig. 54.1 Pin-on-disk wear test setup. **a** Abrasive type and **b** adhesive type

Table 54.1 Pin-on-disk wear test conditions

	Abrasive wear test	Adhesive wear test
Counter body	SiC abrasive disk (Ra = 15 μm)	Hardened steel (HRC 58)
Track wear radius (D) (mm)	75	75
Sliding speed (V) (mm/s)	260	1000
RPM	66	250
Test duration (T) (min)	5	10

worn surfaces was also carried out to study the wear characteristics under different test conditions.

54.3 Results and Discussion

54.3.1 Sliding Abrasive Wear Test

After the wear test, the height loss was calculated and recorded in Table 54.2. Figure 54.2 represents comparative height loss of NiTi–W-coated pins under various normal load conditions and uncoated Ti–6Al–4V alloy pin (tested at 5 N load) after the abrasive wear test. The graph clearly shows that the reduction of the height of the NiTi–W-cladded pins is significantly lower than the Ti–6Al–4V alloy pin. For 5 N load, the height loss of the Ti–6Al–4V alloy pin was found almost eleven times higher than NiTi–W coating. It may also appear that the wear of uncoated Ti–6Al–4V

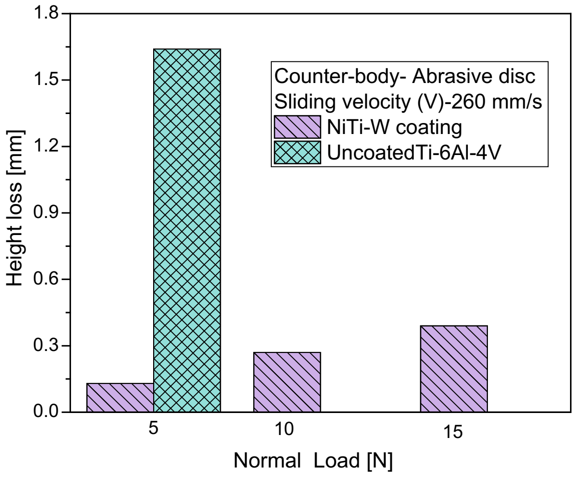

Fig. 54.2 Comparison of wear or height loss of the NiTi–W-coated pins and uncoated Ti–6Al–4V alloy pin after the wear test for various applied normal load

Table 54.2 Calculation of height loss for sliding abrasive wear test

Sample	Load (N)	Initial height of pin (mm)	Final height of pin (mm)	Height loss (mm)
NiTi–W-coated Ti–6Al–4V pin	5	5.66	5.51	0.15
	10	5.69	5.37	0.32
	15	5.67	5.28	0.39
Uncoated Ti–6Al–4V pin	5	5.22	3.58	1.64

alloy pin at 5 N load is also higher than the wear of coated pins performed at 10 or 15 N normal load.

These wear data signifies a considerable improvement in the wear value for deposition of NiTi–W coating on the Ti–6Al–4V alloy. The plot clearly shows that with an increase of normal load, the wear value of the coated pin gradually increases during the abrasive wear test. Further, the wear or height loss recorded directly by the data acquisition system was also plotted against the test time for the NiTi–W-coated pin under three different normal load conditions (5, 10, and 15 N), and for the Ti–6Al–4V alloy pin for 5 N normal load as illustrated in Fig. 54.3. From the plots, it is evident that the wear or height loss for all the samples increases gradually with the test time. However, depending on the applied normal load the rate of wear varyies, and it is revealed that for the enhancement of the applied load, the rate of wear increases considerably and higher final wear value is obtained for the high normal load. Figure 54.3b which represents the wear plot for Ti–6Al–4V alloy

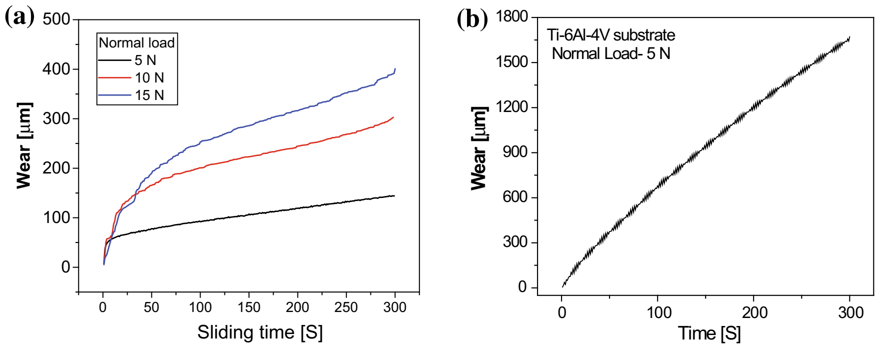

Fig. 54.3 Wear or height loss of **a** NiTi–W-coated Ti–6Al–4V pin for different normal loads (5, 10, and 15 N), **b** uncoated Ti–6Al–4V pin for 5 N

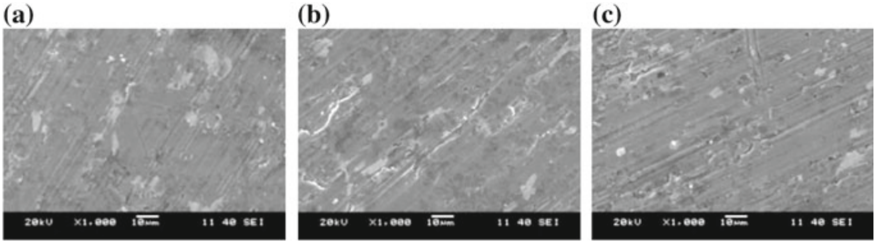

Fig. 54.4 SEM images of worn surfaces of the NiTi–W-coated Ti–6Al–4V pin after the wear test under different normal loads **a** 5, **b** 10, and **c** 15 N

pin shows a drastically higher wear rate and final wear value than that obtained for NiTi–W-coated Ti–6Al–4V alloy pin samples.

Figure 54.4 depicts the SEM images of worn surfaces of the NiTi–W-coated Ti–6Al–4V pin for employing various normal loads. From the images, it is noticed that at lower normal load (5 N), the scratch intensity on the worn out surface, which was created during the sliding of abrasive particles against the coated sample is relatively less. However, with the augmentation of normal load, the scratch intensity on the worn-out surface increases. Thus, there is an enhancement in the wear rate or overall wear is observed to increase with the employed load.

54.3.2 Sliding Adhesive Wear Test

Similarly sliding adhesive wear test was also performed on the pin-shaped coated as well as uncoated samples. However, after the test, the height loss was measured for both NiTi–W-coated and uncoated Ti–6Al–4V alloy pin and recorded as demonstrated in Table 54.3. Figure 54.5 represents the height loss of the NiTi–W-coated

Table 54.3 Calculation of height loss for adhesive wear

Sample	Load (N)	Initial height of pin (mm)	Final height of pin (mm)	Height loss (mm)
NiTi–W-coated Ti–6Al–4V pin	10	5.61	5.594	0.016
	20	5.64	5.612	0.028
	30	5.67	5.614	0.048
Uncoated Ti–6Al–4V pin	10	5.51	5.47	0.04
	20	5.65	5.51	0.14
	30	5.63	5.29	0.34

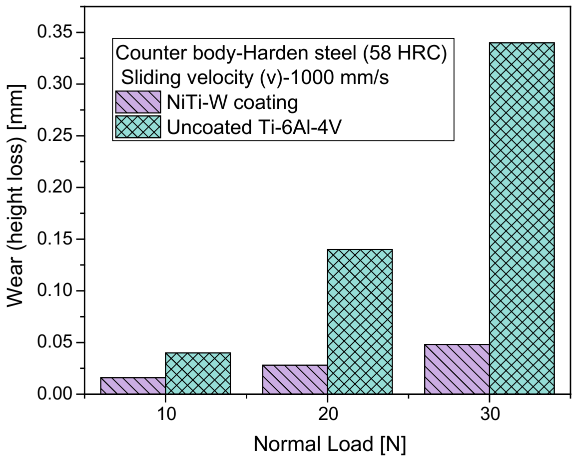

Fig. 54.5 Comparison of wear or height loss of the NiTi–W-coated pins and Ti–6Al–4V alloy pin after the adhesive wear test under different normal load conditions

pins and Ti–6Al–4V alloy pins after the sliding wear test against the hardened steel disk (HRC 58) under different normal load conditions as measured by a Vernier caliper. From the plot, it is clearly evident that the height losses of the NiTi–W-coated Ti–6Al–4V alloy pins are reasonably lower than the uncoated pin for all different normal load conditions. Comparing the wear values with the sliding abrasive wear as plotted in Fig. 54.2, it can be distinctly seen that the sliding wear against the hardened steel plate is much lower (almost ten times) than the sliding wear test performed against the abrasive disk, even when the tests against the hardened steel plate were performed at higher sliding velocity, higher normal load, and for a longer duration. The wear of the uncoated Ti–6Al–4V alloy was also found to be relatively lower compared to the wear value attained against the abrasive disk. For both NiTi–W coating and uncoated Ti–6Al–4V alloy pins, an incremental wear value was recorded for increasing the normal load from 10 to 30 N.

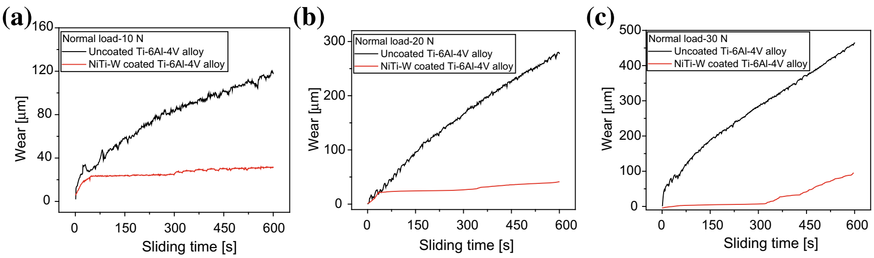

Fig. 54.6 Comparison of adhesive wear between NiTi–W-coated Ti–6Al–4V pin and uncoated Ti–6Al–4V pin for different normal loads **a** 10, **b** 20, and **c** 30 N

The aggregate wear or height loss for the NiTi–W-coated pin, and Ti–6Al–4V alloy was also recorded through a data acquisition system and compared for different normal load conditions (10, 20, and 30 N) as illustrated in Fig. 54.6a–c. The plots show that the cumulative wear for both NiTi–W-coated pin and uncoated Ti–6Al–4V alloy pin samples increases gradually with the sliding time for all different applied normal load conditions. However, the rate of wear for the uncoated pin sample is much higher than the NiTi–W-coated pin samples. It is also noted that with the enhancement of the employed normal load, the wear rates, as well as the final wear values, were increased considerably.

Figure 54.7 shows the SEM images of the NiTi–W-clad surface after the adhesive wear test under a normal load of 10, 20, and 30 N for using the sliding velocity of 1000 mm/s. The images show that at lower normal load, the worn surface is very smooth, without any scratches. However, with the increase of load, it is evident that some scratches are formed, which is probably created due to the removal of coating material and subsequent action of those particles on the coated surface at higher load. Hence, the wear value of the coated pin amplified with the rise of the employed normal load.

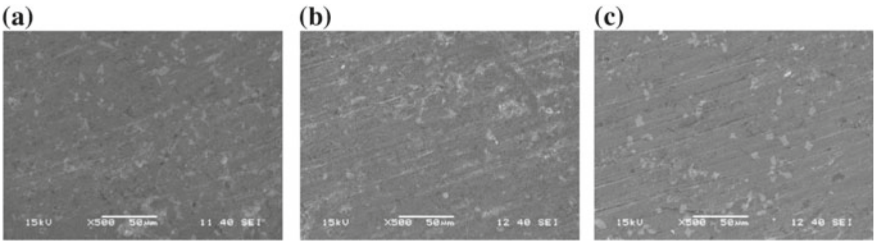

Fig. 54.7 SEM images of worn surfaces of the NiTi–W-coated Ti–6Al–4V pin after the sliding adhesive wear test under different normal loads **a** 10, **b** 20, and **c** 30 N

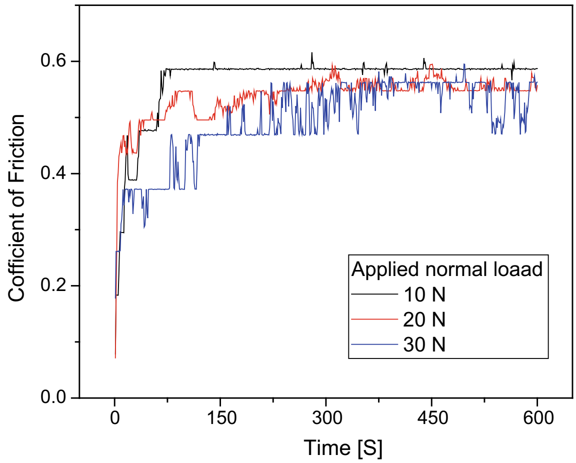

Fig. 54.8 Coefficient of friction of NiTi–W coating against the hardened steel (HRC 58) for different normal loads **a** 10, **b** 20, and **c** 30 N

54.3.3 COF for Adhesive Wear

In addition, during the sliding adhesive wear test, the coefficient of friction of the coated samples wear was also noted. Figure 54.8 depicts the coefficient of friction (COF) of NiTi–W coating as recorded with respect to the test time against the hardened steel disk (HRC 58) for different normal load conditions (10, 20, and 30 N). The plots show that the steady-state COF of the NiTi–W composite coating is in the range of 0.54–0.58.

54.4 Conclusions

From the present experimental analysis, the following conclusions can be made.

- The NiTi–W composite coating fabricated on Ti–6Al–4V alloy improves the wear resistance of the substrate material significantly against both, the sliding abrasive disk (abrasive wear) and the hardened steel disk (adhesive wear).
- The NiTi–W composite coating shows up to eleven times better wear resistance than the uncoated Ti–6Al–4V alloy under abrasive wear test condition and more than seven times better under sliding adhesive test condition.
- The sliding abrasive wear performance of the coating is much higher than the wear test carried out against the hardened steel plate.
- The steady-state COF of the NiTi–W composite coating developed by TIG cladding route was found in the range of 0.54–0.58.

References

1. Molinria, A., Straffelinia, G., Tesia, B.: Dry sliding wear mechanisms of the Ti-6Al-4V alloy. Wear **208**, 105–112 (1997)
2. Banerjee, D., Williams, J.C.: Perspectives on titanium science and technology. Acta Mater. **61**, 844–879 (2013)
3. Waghmare, D.T., Padhee, C.K., Prasad, R., Masanta, M.: NiTi coating on Ti-6Al-4V alloy by TIG cladding process for improvement of wear resistance: microstructure evolution and mechanical performances. J. Mater. Process. Technol. **262**, 551–561 (2018)
4. Kustas, F.M., Misra, M.S.: ASM Handbook: Friction and Wear of Titanium Alloys. ASM International (1991)
5. Galvan, D., Ocelík, V., Pei, Y., Kooi, B.J., De Hosson, J.T.M., Ramous, E.: Microstructure and properties of TiB/Ti-6Al-4V coatings produced with laser treatments. J. Mater. Eng. Perform. **13**, 406–412 (2004)
6. Lin, Y.H., Lei, Y.P., Li, X.Q., Zhi, X.H., Fu, H.G.: A study of TiB_2/TiB gradient coating by laser cladding on titanium alloy. Opt. Lasers Eng. **82**, 48–55 (2016)
7. Buytoz, S., Ulutan, M.: In situ synthesis of SiC reinforced MMC surface on AISI 304 stainless steel by TIG surface alloying. Surf. Coat. Technol. **200**, 3698–3704 (2006)
8. Saroj, S., Sahoo, C.K., Masanta, M.: Microstructure and mechanical performance of TiC-Inconel825 composite coating deposited on AISI 304 steel by TIG cladding process. J. Mater. Process. Technol. **249**, 490–501 (2017)
9. Gao, F., Wang, H.M.: Dry sliding wear property of a laser melting/deposited Ti_2Ni/TiNi intermetallic alloy. Intermetallics **16**, 202–208 (2008)
10. Sahoo, C.K., Masanta, M.: Microstructure and mechanical properties of TiC-Ni coating on AISI304 steel produced by TIG cladding process. J. Mater. Process. Technol. **240**, 126–137 (2017)